IEEE Access
Multidisciplinary | Rapid Review | Open Access Journal

Received February 1, 2018, accepted May 11, 2018, date of publication May 25, 2018, date of current version June 26, 2018.

Digital Object Identifier 10.1109/ACCESS.2018.2839699

Rainfall Estimation Based on the Intensity of the Received Signal in a LTE/4G Mobile Terminal by Using a Probabilistic Neural Network

FRANCESCO BERITELLI[1], GIACOMO CAPIZZI[1], GRAZIA LO SCIUTO[1], CHRISTIAN NAPOLI[2], AND FRANCESCO SCAGLIONE[1]

[1]Department of Electrical, Electronic and Informatics Engineering, University of Catania, 95125 Catania, Italy
[2]Department of Mathematics and Computer Science, University of Catania, 95125 Catania, Italy

Corresponding author: Francesco Beritelli (francesco.beritelli@dieei.unict.it)

ABSTRACT Rainfall estimation based on the impact of rain on electromagnetic waves is a novel methodology that has had notable advancements during the last few years. Many studies conducted on this topic in the past considered only the electromagnetic waves with frequencies greater than 10 GHz since the rainfall impact on the electromagnetic wave attenuation is reduced at lower frequencies. Over the last few years, some authors have demonstrated that there can be a non-negligible attenuation even on the signals received on a global system for mobile communications mobile terminal in presence of rain. In this paper, we propose a new classification method based on a probabilistic neural network to obtain an accurate classification between four rainfall intensities (no rain, weak rain, moderate rain, and heavy rain). The innovative rainfall classification method is based on three received signal level (RSL) local features of the 4G/LTE: the instantaneous RSL, the average RSL value, and its variance calculated by using a sliding window. The proposed method exhibits good performance, obtaining an overall correct classification rate of 96.7%. Almost all papers on this topic present in the literature focus on electromagnetic waves with frequencies greater than 10 GHz, in which the rain impact is more relevant, according to the rain attenuation model. However, only the 4G/LTE signal has such widespread geographic coverage, so the proposed classification method can provide noticeable improvements in the creation of rainfall maps with higher spatial resolution.

INDEX TERMS Feature extraction techniques, LTE, probabilistic neural network, radio signal attenuation, rainfall estimation.

I. INTRODUCTION

Rainfall monitoring is a topic of great importance for several application contexts: hydraulic structure design, agriculture, weather forecasting, climate modeling, etc. Today, the main rainfall measurement methods are rain gauge, weather radar and satellites.

A rain gauge is probably the most widespread rainfall measurement device and can provide an accurate rainfall estimation with a fine temporal resolution; in fact, rain gauges record continuously the rainfall level even with short-time intervals. Unfortunately, rain gauges provide only local information, measuring the rainfall level in the specific geographic location where gauge is installed. The rainfall information in any other point must be obtained by interpolating the available data provided by neighboring rain gauges with the consequence that this information can be affected by a higher error.

To improve the measurement accuracy, it is necessary to increase the number of rain gauges along the territory obtaining a global and more accurate view of the phenomena. Since full coverage by local rain gauges is a very expensive solution, weather radar and satellites represent a good solution to face this challenge.

Weather radar detects rain in the atmosphere by emitting microwave pulses and measuring reflected signals from raindrops, providing high temporal resolution precipitation measurements. The distance to the rain is determined from the round-trip time of radar microwave pulses.

Weather radar has the advantage of monitoring a larger area than a rain gauge and determining the areal distribution

of precipitation; however, it is affected by various types of errors that decrease its accuracy, and it is also very expensive.

Satellite rainfall estimations assure greater spatial and temporal resolution, but the rain intensity estimation is less accurate. For this reason, a satellite rainfall estimation is often used to fill the gaps in radar coverage and to assist with the post-processing of radar outputs [1].

In order to improve the accuracy of the estimates obtained by using the previously mentioned approach, in Lazri *et al.* [2] and Lazri and Ameur [3] have proposed a rainfall estimation technique based on the application of image process algorithms to the images provided by satellites. In particular, a multi-spectral approach is employed, collecting images in different spectral bands.

Lately, many papers have been published proposing alternative methods to estimate the rainfall intensity based on the measurements of the received signal level (RSL) in commercial wireless microwave links [4]–[6].

As known from the literature, electromagnetic waves are attenuated in presence of rain, and many rain prediction models are based on this phenomenon.

Many studies conducted on this topic in the past considered only electromagnetic waves with frequencies greater than 10 GHz, since the rainfall impact on the electromagnetic wave attenuation is reduced at lower frequencies. Only a few papers have analyzed the impact of the rain on the cellular system performance, highlighting that even in these circumstances, it is possible to formulate a rain level prediction based on the electromagnetic wave attenuation in presence of rain [7], [8]. In particular, Fang and Yang [9] in a test campaign conducted in Taiwan have demonstrated that there can be a noticeable attenuation in the received signal on a LTE mobile terminal in the presence of rain. This experimental evidence is in contradiction with the attenuation model provided by ITU-R [10].

Brito *et al.* [11] used a data mining technique to select among the data collected from mobile devices on a rainfall alert system suitable for rainfall estimations. To classify the rainfall events, some classification algorithms such as k-nearest neighbors, support vector machine (SVM) and decision tree methodologies were adopted.

Beritelli *et al.* [12] proposed the first approach to rainfall estimation based on the study of the RSL in an Long-Term Evolution (LTE) mobile terminal, adopting a sliding window filter to calculate the mean value and variance.

In this paper, we propose a new classification method based on a probabilistic neural network to obtain a more accurate classification of four rainfall intensities (no-rain, weak rain, moderate rain and heavy rain).

After this introductory section, the paper is structured as follows: Section II provides an overview of some rain attenuation models. Section III describes the testbed scenario and the dataset structure, while Section IV provides the description of the feature extraction process and the classical threshold classification method. Section V illustrates the adopted neural network and its rainfall classification performance, whereas Section VI presents a comparison with some other methods and, finally, Section VII draws conclusions.

II. THE IMPACT OF RAINFALL ON RADIO PROPAGATION

Methods for rain estimates based on radio propagation attenuation can be grouped in two categories: physical and empirical methods.

Physical methods are theoretical (analytic) models that attempt to describe the attenuation on radio propagation due to rain [13], [14]. On the other hand, the empirical methods are based on a database containing real measurements originating from stations located in different climatic zones and consist of simple mathematical expressions obtained by simple interpolations on these data.

Because in many circumstances not all the input parameters required by the analytical models are available, empirical methods are most commonly used. In fact, the rain attenuation model proposed by the International Telecommunication Union for the Radiocommunication (ITU-R) is an empirical model that makes use of the following power-law formula [10]:

$$\gamma_R = k \cdot R^{\alpha} \tag{1}$$

where γ_R (dB/km) is the specific attenuation and R (mm/h) is the rain rate.

The total attenuation A (dB) due to the rain rate R in a radio propagation link of length L can be calculated as:

$$A = L \cdot \gamma_R \tag{2}$$

The empirical coefficients k (k_H for horizontal polarization, k_V for vertical polarization) and α (α_H for horizontal polarization, α_V for vertical polarization) are calculated as functions of frequency f (GHz) in the range from 1 to 1000 GHz and are displayed in appropriates tables in [10].

The relationship between the rain rate and electromagnetic wave attenuation provided by the equation (1) is an empirical approximation. In fact, the exact relationship depends on a number of other parameters such as frequency, temperature, drop size distribution (DSD), etc. However, in most cases, equation (1) provides a good estimate [5].

In this work we presented a novel methodology in order to move beyond the limits of both the theoretical and empirical approach. The adopted solution makes use of a novel feature extraction approach and a neural classifier that is capable to devise the underlying model without a priori assumptions. The model, presented in the following, has been extensively tested on field data.

III. THE TESTBED SCENARIO

A. THE TEST CAMPAIGN

The test campaign was conducted by using a smartphone with a dedicated application, called G-Mon, able to export in CVS format a complete report during time regarding several network and signal parameters such as the received signal strength indicator (RSSI), the reference signal received power (RSRP), the reference signal received quality (RSRQ),

the signal-to-noise ratio (SNR), the location area code (LAC), the cell ID (CID), and the connection type (LTE, HSPA, UMTS, etc.). More specifically we have analyzed the RSSI to evaluate the attenuation and the signal fluctuation. The knowledge of the cell ID is very important because it allows the verification of if the measured RSL is referred to the same base station. The application allows the collection of data with a programmable frequency. For this experiment, the data were recorded at a frequency of 60 seconds.

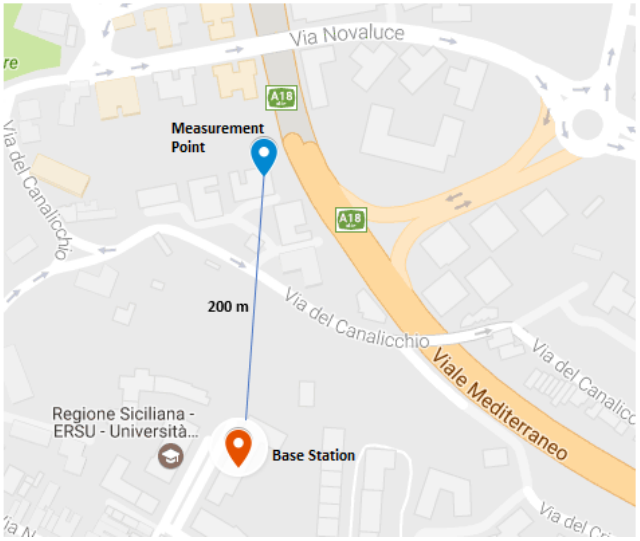

FIGURE 1. Test-bed scenario.

To perform the calibration of the proposed experimental apparatus we proceeded as follows: we placed four mobile terminals (same models and software) in four different locations, each of them connected to the same base station (see Fig. 1). Three mobile terminals, indicated with a dashed line in the figure, were used to calculate the considered features of the RSL, i.e. average value and variance, in no-rain conditions, in order to calibrate the system and then normalize the collected RSL values at different rainfall levels compared to the no-rain condition. In order to establish a database the mobile terminal with the dedicated measurement application was located at approximately 200 m from the base station in a way that the two points were in direct visibility. To relate the data collected by mobile terminal with the real rain rate a ''tipping bucket rain gauge'' placed at the same location of the mobile terminal was used. Instead of weather station date, due to their possible scarceness in other locations, as well as their unpredictable density, we preferred this solution due to its locality with respect to the collected data.

The tipping bucket rain gauge includes a rain-collecting funnel, two triangular vessels mounted on a fulcrum, and an electronic switch. Rain is channeled through the funnel to one of the vessels. When the vessel is full, it becomes overbalanced and tips down, emptying itself into the outer shell of the gauge, as the other vessel is raised to a position for the next reading.

To devise the proposed classification method, we have created a database with the collected data. The database includes power measurements collected in four different weather conditions: no rain, weak rain, moderate rain, and heavy rain. The database was divided into three groups: a training set, a validation set and a test set. The database composition is displayed in Table 1.

TABLE 1. Database composition.

Rain Classification	Training	Validation	Test
No Rain	2400	1440	960
Weak Rain	310	186	124
Moderate Rain	405	243	162
Heavy Rain	265	159	106

B. DATA ANALYSIS

In this subsection, we will analyze the statistical properties of the data collected in the database to discover those properties that have discriminant power for the classification.

For our purposes, we will classify rainfall levels according to the criteria shown in Table 2.

TABLE 2. Rainfall classification criteria.

Rain Classification	Precipitation Intensity (mm/h)
No Rain	0
Weak Rain	< 2.5
Moderate Rain	$2.5 - 5$
Heavy Rain	$6 - 10$
Very Heavy Rain	$11 - 30$
Cloudburst	> 30

Fig. 2 outlines samples of the RSL in different rainfall conditions, while Fig. 3 represents the density probability distributions of the RSL at various rainfall conditions.

The analysis of the probability density distributions (pdfs) shown in Fig. 3 indicates that in different rain conditions, i.e., no rain, weak rain, moderate rain and heavy rain, the pdf of the RSLs has a different value for the mean and variance. Therefore, the use of the local values of these quantities can be effective for rainfall classification. In fact, it is clear that there is a significant difference in the local average values of the RSLs between the rain and no-rain conditions. Therefore, by using only the local average values of the RSLs, we can discriminate between rain and no-rain conditions. Unfortunately, the local average values of the RSLs are not sufficient to discriminate between weak, moderate and heavy rain. To distinguish between these three rainfall conditions, it is sufficient to observe that (see Fig. 3) weak, moderate and heavy rainfalls present different local variance values.

In order to recognize and classify the rainfall levels, in this paper, we use three RSL local features: the RSL

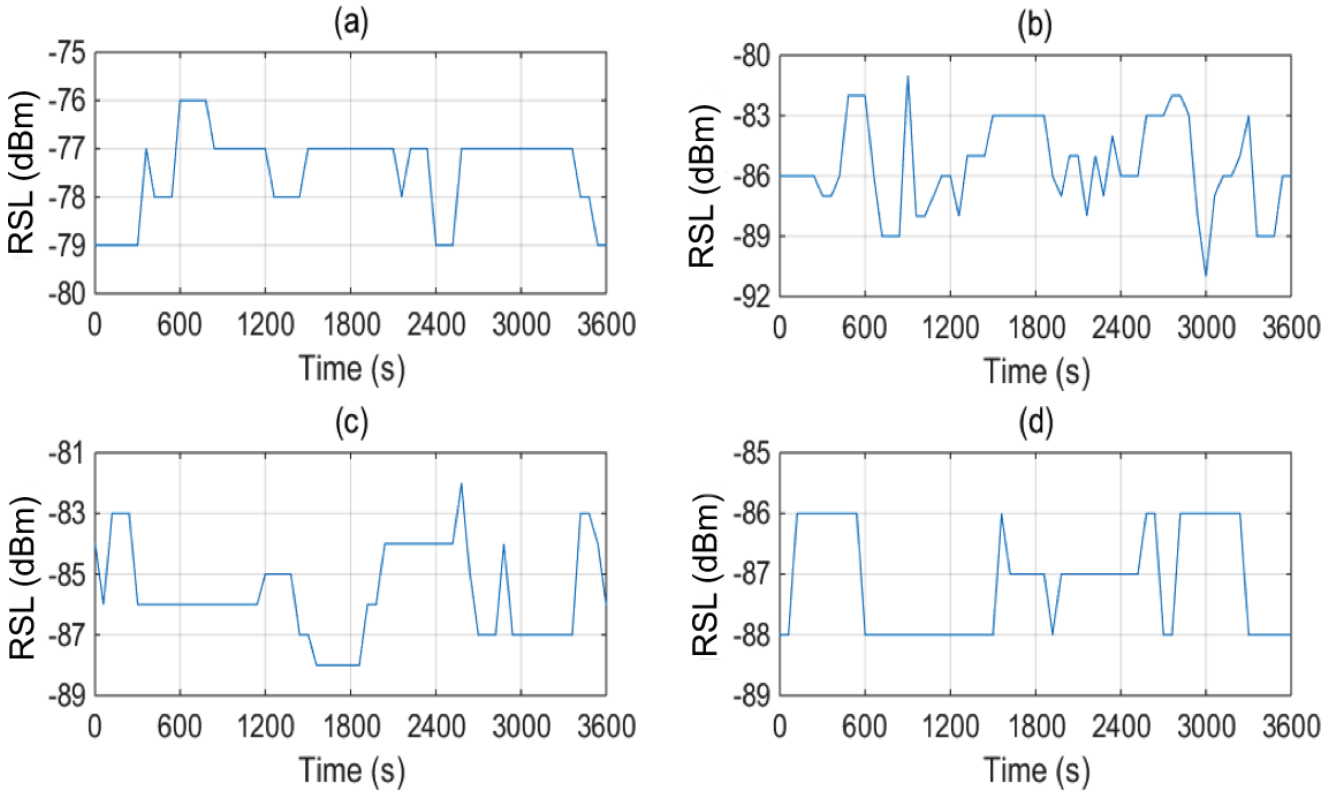

FIGURE 2. A sample of the received signal level for a 1 hour duration in different rain conditions: (a) No rain, (b) weak, (c) moderate and (d) heavy rain conditions.

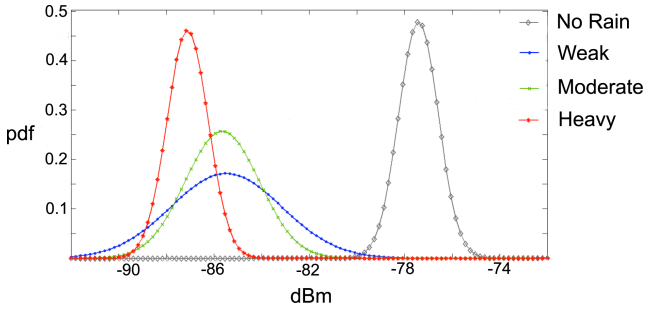

FIGURE 3. Probability density distributions of the RSLs for no-rain, light rain, moderate rain, and heavy rain.

instantaneous, the RSL average value and its variance. These last two are calculated by using a sliding window.

The next section will briefly examine the effect of the window size on the misclassification error. However, there are several factors that can affect the received signal features, e.g. the distance from the base station to the mobile terminal, obstacles, fading, etc.

To observe rain effects, we need to differentiate between any impact not due to the precipitation and the impact caused by the precipitation phenomena. For this reason we need to calibrate the system by measuring the RSL data in no-rain conditions in order to calculate the reference RSL level that includes the impact of all attenuation sources except the rain; once the reference level is calculated, all the measured RSL values must be normalized as shown by the equation :

$$RSL_n = RSL_m / RSL_{nr} \tag{3}$$

where:

- RSL_n is the normalized RSL
- RSL_m is the measured RSL
- RSL_{nr} is the average RSL measured in no-rain conditions

The idea is to geolocalize the collected RSL data in order to identify the maximum area in which the RSL is almost constant and then normalize all the collected RSL data in this area.

IV. FEATURE EXTRACTION

Considering the three critical rainfall conditions (weak, moderate, heavy), the first analysis of the misclassification errors, where the sliding window size changes, is focused on the minimization of the probability error of the variance calculated using the window. By considering the problem of a weak-moderate classification, the error probability in relation to a fixed window size for a weak rain is:

$$P_{e,w}(t) = P(v_w < t) = \int_{-\infty}^{t} \frac{1}{\sigma_w \sqrt{2\pi}} e^{\frac{-(v_w - \mu_w)^2}{2\sigma_w^2}} dv_w \tag{4}$$

while the error probability for a moderate rain is:

$$P_{e,m}(t) = P(v_m > t) = \int_t^{-\infty} \frac{1}{\sigma_m\sqrt{2\pi}} e^{\frac{-(v_m-\mu_m)^2}{2\sigma_m^2}} dv_m \quad (5)$$

where:

- v_w and v_m are the variance vectors for weak and moderate rain, respectively.
- σ_w and σ_m are the standard deviations of v_w and v_m.
- μ_w and μ_m are the mean values of v_w and v_m
- t is the weak-moderate threshold.

The total error probability in the weak-moderate rain classification is given by:

$$\begin{aligned} P_{e,w-m}(t) &= P_{e,w}(t) + P_{e,m} \\ &= \int_{-\infty}^{t} \frac{1}{\sigma_w\sqrt{2\pi}} e^{\frac{-(v_w-\mu_w)^2}{2\sigma_w^2}} dv_w \\ &\quad + \int_t^{-\infty} \frac{1}{\sigma_m\sqrt{2\pi}} e^{\frac{-(v_m-\mu_m)^2}{2\sigma_m^2}} dv_m \end{aligned} \quad (6)$$

while the total error probability in the moderate-heavy rain classification is given by:

$$\begin{aligned} P_{e,m-h}(t) &= P_{e,m}(t) + P_{e,h} \\ &= \int_t^{-\infty} \frac{1}{\sigma_m\sqrt{2\pi}} e^{\frac{-(v_m-\mu_m)^2}{2\sigma_m^2}} dv_m \\ &\quad + \int_{-\infty}^{t} \frac{1}{\sigma_h\sqrt{2\pi}} e^{\frac{-(v_h-\mu_h)^2}{2\sigma_h^2}} dv_h \end{aligned} \quad (7)$$

By minimizing the error probabilities described by equations (6) and (7) with respect to the threshold and the window size, we obtained a sliding window size of 30 samples.

Fig. 4 shows the normalized variance values of RSL for the three rainfall conditions (weak, moderate, heavy) calculated by using two sliding windows of two different sizes: (a) 15 and (b) 30 samples. The figure also shows the two thresholds that minimize equations (6) and (7).

Analyzing Fig. 4, we observe that when using a sliding window size of 15 samples, there is an overlap between the curves representing moderate and heavy rain conditions, whereas such an overlap does not occur when we use a sliding window size of 30 samples. Only by using a sliding window size of 30 samples can we correctly classify the three rainfall conditions (weak, moderate, heavy).

Considering the discrimination thresholds obtained by minimizing the error probabilities described by equations (6) and (7), we obtain a total misclassification error of 15% (with a sliding window size of 30 samples) due to weak and moderate rainfall ratings, while no-rain and heavy rain conditions are always properly classified.

This approach provides good performance in terms of the misclassification error rate, especially for the heavy rain recognition, but it is based only on the variance values, a parameter that can be influenced by other fading factors.

To improve the robustness of the method and reduce its misclassification error, the authors of the paper propose a neural network-based approach that makes use of three features: the RSL instantaneous value, the RSL average and its variance.

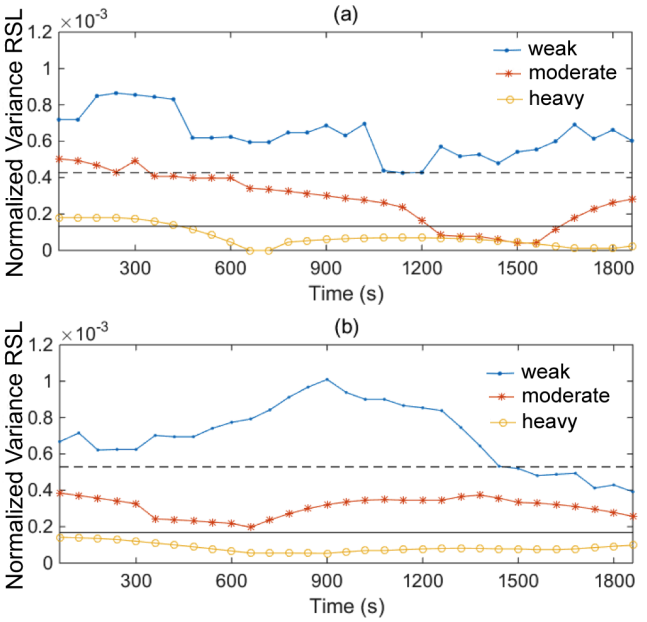

FIGURE 4. The normalized RSL variance values for the three rainfall levels using two different window sizes: (a) 15 and (b) 30 samples.

V. THE PROPOSED NEURAL CLASSIFIER

A. THE SELECTED PNN

The proposed classifier is based on a probabilistic neural network (PNN) that is designed and trained to provide a correct classification of four rainfall conditions: clear weather and weak, moderate and heavy rainfall. The dataset was obtained under sunshine and under weak, moderate and heavy rain, according to the rainfall classification proposed in Table 1.

A PNN is related to Parzen window pdf estimator [15]–[20]. Moreover, a PNN consists of several subnetworks, each of which is a Parzen window pdf estimator for each of the classes. The input nodes are the input data. The second layer consists of Gaussian functions in which the points of the train set are used as the centers. The third layer performs an average operation of the outputs from the second layer for each class. The fourth layer performs a vote, selecting the largest value. The associated class label is then determined [21]–[23].

When an input data are presented, the input layer spreads this sample to the pattern layer neurons (second layer). In the second layer (pattern layer), each vector input is processed by the function described in the following way:

$$y_k(x(t)) = \sum_{j=1}^{M} w_{k,j}\Phi_j(x(t)) \quad (8)$$

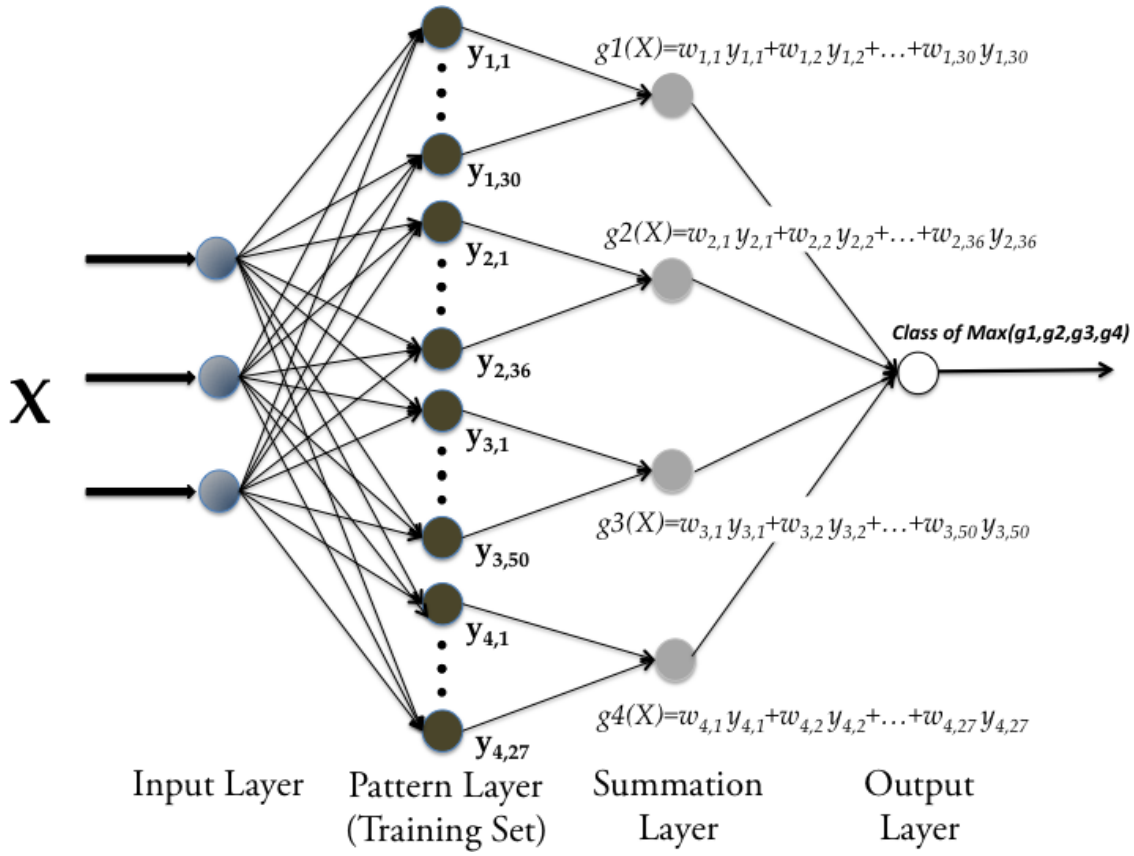

FIGURE 5. The trained PNN classifier used to obtain an accurate classification between four rainfall intensities (weak rain, moderate rain, clear weather and heavy rain).

with

$$\Phi_j(x(t)) = exp\left\{-\frac{1}{2\sigma_j}(x\,(t)-\mu_j)^T\,\Sigma_j^{-1}(x\,(t)-\mu_j)\right\} \quad (9)$$

where ϕ_j (x(t)) is the contribution of the j-neuron in the k-class; y_k is the transfer function and $w_{k,j}$ is the weight of the j-neuron of the k-class.

In the output layer, each input sample is associated with the class with the highest output [24], [25].

In the eq. (9), μ_j and $\sum_j$ are the function center (mean vector) and covariance matrix of the j-th basis function, respectively, and σ_j is a smoothing parameter controlling the spread of the j-th basis function.

For the sake of simplicity, we will assume that $\sum_j$ is diagonal so that we have four global smoothing parameters, $\sigma_1, \sigma_2, \sigma_3$, and σ_4. The parameter σ_1 is used in those basis functions that have centers originating from a weak rain condition; σ_2 is utilized for those functions coming from a moderate rain condition; σ_3 is used for those basis functions that originate from a clear weather condition and σ_4 is used for those functions that come from a heavy rain condition.

The determination of the smoothing parameters is performed by calculating the spreads of the training data set belonging to the reference classes for $\sigma_1, \sigma_2, \sigma_3$, and σ_4.

Adding and removing training samples simply involves adding or removing neurons in the pattern layer, and a minimal retraining is required. For the training of the neural network, simply note that the centers and spreads are predetermined and then only the weights w_{kj} are found.

The calculation can be performed by using the method of least squares.

B. EXPERIMENTAL RESULTS

The dataset used to train and test the PNN consists of more than 112 hours of data collected every minute. More precisely, the dataset is organized as follows: 4800 samples for no-rain condition, 620 for weak rain, 810 for moderate rain, and 530 for heavy rain.

The training set has been drawn out from the entire dataset randomly by choosing 2400 samples for the no-rain condition, 310 samples for the weak rain, 405 samples for the moderate rain and 265 samples for the heavy rain. While the validation set has been randomly drawn from the remaining dataset; and after that, the entire dataset has been drawn out of the training set. The remaining samples were used to form the test set that was used to evaluate the pattern recognition algorithm. The compositions of the training, validation and test sets are shown in Table 1.

TABLE 3. Rainfall classification methods comparison.

	Method	Features	Classifier	No-Rain %	Rain %	Weak %	Moderate %	Heavy %
Brito et al. [9]	GSM signal	RSL	SVM	82.84	84.79	75.78	n.d.	88.26
Guo et al. [24]	Sound in vehicle	Frequency domain (Spectral centroid, Mel frequency Cepstral coefficient Etc.)	Decision Tree Random Forest Naive Bayes Multi-layer Perceptron k-NN SVM	95.43 95.11 90.57 98.55 94.48 92.88	95.15 98.46 95.54 99.02 98.13 97.13	n.d. n.d. n.d. n.d. n.d. n.d.	n.d. n.d. n.d. n.d. n.d. n.d.	n.d. n.d. n.d. n.d. n.d. n.d.
Cheakassky et al. [25]	Commercial Microwave link	Signal attenuation	KFD (kernel Fisher discriminant)	96.74	80.18	n.d.	n.d.	n.d.
The proposed method	4G/LTE signal attenuation	RSL instantaneous value, RSL average and its variance.	PNN	100	n.d.	90	96.7	100

The training set is used to find the model parameters in the used PNN network. These parameters are the number of neurons for each class (weak rain, moderate rain, clear weather and heavy rainfall), the smoothing parameters σ_1, σ_2, σ_3, and σ_4, and the weight values.

The smoothing parameters are calculated as described in the previous subsection, while the calculus of the optimal number of neurons and the determination of their centroids are described below:

1) If we use the samples of the training set as neuron centers, then we will obtain a layer pattern of 3380 neurons split up into four classes (2400 neurons for the no-rain, 310 neurons for the weak rain, 405 neurons for the moderate rain and 265 neurons for the heavy rain conditions).

By applying the least squares method on the training set, we compute the weights $w_{k,j}$.

2) We trim the neuron that has the lowest weight and compute the network's weights again by using the validation set. This phase of the training process stops when the error, in terms of correct classification on the validation set, exceeds 1% with respect to the previous step.

The obtained network after the training is shown in Fig. 5. In the pattern layer, there are 143 remaining neurons (30 of them are related to the weak rain condition, 36 are related to moderate rain, 50 are related to clear weather, and 27 are related to the heavy rainfall condition).

The trained PNN classifier was used on the test set, and a misclassification error of 3.3% was obtained. This error is because the network, under very difficult conditions, confuses light rainfall with the moderate rainfall. More specifically, the analysis of the confusion matrix obtained with the outputs of the classifier, when applied on the test set, shows (see Fig. 6) that the misclassification error equals 1.1% because the network confuses moderate rainfall with light rainfall. The remaining misclassification error of 2.2% is because the network confuses the light rainfall with moderate rainfall, while the clear weather and heavy rainfall conditions are always properly classified.

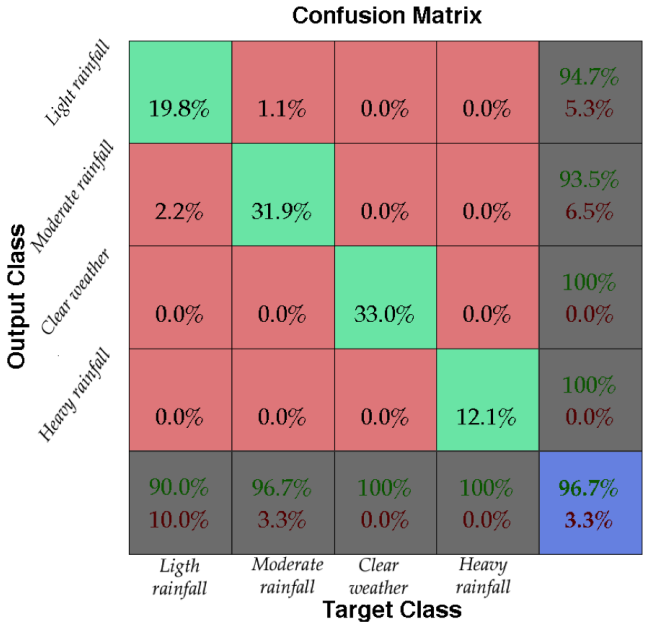

FIGURE 6. Confusion matrix relative to the results of the classification between the four rainfall intensities (light rainfall, moderate rainfall, clear weather and heavy rainfall) obtained by using the PNN classifier.

Because this classification method provides good performance with a correct classification rate of 96.7%, it can provide noticeable improvements in the building of rainfall maps with higher spatial resolution thanks to the high geographic coverage of the 4G/LTE signal.

VI. PERFORMANCE COMPARISON

To the best of our knowledge, except for a preliminary study by Beritelli *et al.* [12] there are no papers in the literature based on 4G/LTE signal attenuation in the presence of rainfall. Almost all papers on this topic, presented in the literature, are based on the rain attenuation analysis of the electromagnetic waves with frequencies higher than 10 GHz,

where the rain impact is more relevant according to the rain attenuation models.

Even if at frequencies higher than 10 GHz, all the rainfall classification methods perform better because of the higher impact of the rain on the radio propagation at this frequency. Table 3 summarizes some of the most popular rainfall classification methods operating at these frequencies and compares the performance with the classification method proposed by the authors.

By analyzing the Table 3, we can state that even when some of the other methods seem to outperform our method for one measurement, looking at the overall classification performance, the results of the proposed method are definitively better. Furthermore, it is the only method that can discriminate between weak rainfall, moderate rainfall and heavy rainfall. Finally, it should also be noted that other methods operate at frequencies higher than 10 GHz, so in comparison, they have an advantage.

VII. CONCLUSION

In this paper we presented an novel rainfall classification system based on RSL local features extracted from 4G/LTE signal parameters: instantaneous RSL, average RSL value and variance, which has been calculated by means of a sliding window. The classifier system has been provided by implementing a PNN in order to recognize the different precipitation levels. The classification system has been designe to consider four possible rainfall classes: no-rain, weak, moderate and heavy rain. Such classes has been defined accordingly to the criteria shown in Table 2.

The proposed method obtained satisfactory performances, with an overall rate of correct classifications of 96.7%.

It should be highlighted that the proposed approach is not limited by any band-related constraint, therefore it could be applied for all the LTE/4G frequency bands.

On the countrary, the major part of the papers presented in the literature on this topic have set their focus on electromagnetic waves within a frequency range over 10 GHz, in which the rain impact is more relevant, according to the rain attenuation model. However, only the 4G/LTE signal has such widespread geographic coverage, so the proposed classification method can provide noticeable improvements in the creation of rainfall maps with higher spatial resolution.

In an application context the 4G/LTE receiver can be located in each base station and forced to connect to the nearest neighbor cell, ensuring a minimum distance between the transmitter and the receiver to guarantee an adequate rain impact on the signal propagation.

REFERENCES

[1] S. Kevin, *Flash Floods: Forecasting and Warning*. Dordrecht, The Netherlands: Springer, 2012.

[2] M. Lazri, Z. Ameur, S. Ameur, Y. Mohia, J. M. Brucker, and J. Testud, "Rainfall estimation over a Mediterranean region using a method based on various spectral parameters of SEVIRI-MSG," *J. Adv. Space Res. Elsevier*, vol. 52, no. 8, pp. 1450–1466, 2013. [Online]. Available: http://dx.doi.org/10.1016/j.asr.2013.07.036

[3] M. Lazri and S. Ameur, "Combination of support vector machine, artificial neural network and random forest for improving the classification of convective and stratiform rain using spectral features of SEVIRI data," *Atmos. Res.*, vol. 203, pp. 118–129, May 2018. [Online]. Available: https://doi.org/10.1016/j.atmosres.2017.12.006

[4] A. Overeem, H. Leijnse, and R. Uijlenhoet, "Country-wide rainfall maps from cellular communication networks," *Proc. Nat. Acad. Sci. USA*, vol. 110, no. 8, pp. 2741–2745, Feb. 2013.

[5] H. Messer and L. Gazit, "From cellular networks to the garden hose: Advances in rainfall monitoring via cellular power measurements," in *Proc. IEEE Global Conf. Signal Inf. Process. (GlobalSIP)*, Washington, DC, USA, Dec. 2016, pp. 1012–1016.

[6] J. Ostrometzky and H. Messer, "Accumulated rainfall estimation using maximum attenuation of microwave radio signal," in *Proc. IEEE 8th Sensor Array Multichannel Signal Process. Workshop (SAM)*, A Coruña, Spain, Jun. 2014, pp. 193–196.

[7] A. Sharma and P. Jain, "Effects of rain on radio propagation in GSM," *Int. J. Adv. Eng. Appl.*, vol. 1, pp. 83–86, Jan. 2010.

[8] K. Vijay, "Effect of environmental parameters on GSM and GPS," *Indian J. Sci. Technol.*, vol. 7, no. 8, pp. 1183–1188, 2014.

[9] S.-H. Fang and Y.-H. S. Yang, "The impact of weather condition on radio-based distance estimation: A case study in GSM networks with mobile measurements," *IEEE Trans. Veh. Technol.*, vol. 65, no. 8, pp. 6444–6453, Aug. 2016.

[10] *Specific Attenuation Model for Rain for Use in Prediction Methods*, document ITU-R P.838-3, ITU-R Recommendation, 2005.

[11] A. Brito, L. Fernando, and M. Keese Albertini, "Data mining of meteorological-related attributes from smartphone data," *INFOCOMP, J. Comput. Sci.*, vol. 15, no. 2, pp. 1–9, 2016.

[12] F. Beritelli, G. Capizzi, G. Lo Sciuto, F. Scaglione, D. Polap, and M. Woźniak, "A neural network pattern recognition approach to automatic rainfall classification by using signal strength in LTE/4G networks," in *Proc. Int. Joint Conf. Rough Sets*, 2017, pp. 505–512.

[13] J. S. Ojo, M. O. Ajewole, and S. K. Sarkar, "Rain rate and rain attenuation prediction for satellite communication in Ku and Ka bands over Nigeria," *Prog. Electromagn. Res. B*, vol. 5, pp. 207–223, 2008.

[14] M. C. Kestwal, S. Joshi, and L. S. Garia, "Prediction of rain attenuation and impact of rain in wave propagation at microwave frequency for tropical region (Uttarakhand, India)," *Int. J. Microw. Sci. Technol.*, vol. 2014, Jun. 2014, Art. no. 958498.

[15] E. Parzen, "On estimation of a probability density function and mode," *Ann. Math. Stat.*, vol. 33, no. 3, pp. 1065–1076, 1962.

[16] D. F. Specht, "Probabilistic neural networks," *Neural Netw.*, vol. 3, no. 1, pp. 109–118, 1990.

[17] F. Ancona, A. M. Colla, S. Rovetta, and R. Zunino, "Implementing probabilistic neural networks," *Neural Comput., Appl.*, vol. 5, no. 3, pp. 152–159, 1997.

[18] F. Bonanno, G. Capizzi, G. L. Sciuto, and C. Napoli, "Wavelet recurrent neural network with semi-parametric input data preprocessing for micro-wind power forecasting in integrated generation systems," in *Proc. Int. Conf. Clean Elect. Power (ICCEP)*, Taormina, Italy, Jun. 2015, pp. 602–609.

[19] H. Wang, J. Hu, and W. Deng, "Compressing Fisher vector for robust face recognition," *IEEE Access*, vol. 5, pp. 23157–23165, 2017.

[20] L. Cheng, M. F. Ren, and G. Xie, "Multipath estimation based on centered error entropy criterion for non-Gaussian noise," *IEEE Access*, vol. 4, pp. 9978–9986, 2016.

[21] C. Bishop, *Pattern Recognition and Machine Learning* (Information Science and Statistics). New York, NY, USA: Springer, 2006.

[22] B. D. Ripley, *Pattern Recognition and Neural Networks*. Cambridge, U.K.: Cambridge Univ. Press, 2008.

[23] M. M. Gupta, L. Jin, and N. Homma, *Static and Dynamic Neural Networks*. New York, NY, USA: Wiley, 2003.

[24] F. Beritelli, G. Capizzi, G. Lo Sciuto, C. Napoli, and F. Scaglione, "Automatic heart activity diagnosis based on Gram polynomials and probabilistic neural networks," *Biomed. Eng. Lett.*, vol. 8, no. 1, pp. 77–85, 2018. [Online]. Available: https://doi.org/10.1007/s13534-017-0046-z

[25] S. N. Barnea *et al.*, "Photo-electro characterization and modeling of organic light-emitting diodes by using a radial basis neural network," in *Proc. 16th Int. Conf. Artif. Intell. Soft Comput. (ICAISC)*, Zakopane, Poland, Jun. 2017, pp. 378–389.

[26] H. Guo *et al.*, "Tefnut: An accurate smartphone based rain detection system in vehicles," in *Proc. Int. Conf. Wireless Algorithms, Syst., Appl.*, 2016, pp. 13–23.

[27] D. Cherkassky, J. Ostrometzky, and H. Messer, "Precipitation classification using measurements from commercial microwave links," *IEEE Trans. Geosci. Remote Sens.*, vol. 52, no. 5, pp. 2350–2356, May 2014.

FRANCESCO BERITELLI received the Laurea degree in electronic engineering and the Ph.D. degree in electronics, computer science, and telecommunications engineering from the University of Catania, Catania, Italy, in 1993 and in 1997, respectively. From 1997 to 2000, he took an active part in international ITU-T standardization meetings in collaboration with CSELT (now Telecom Italia LAB). Since 1998, he has been a Founding Member of the Multimedia Technologies Institute-MTI, applied research laboratory operating in digital signal processor and computer telephony integration applications. Since 2002, he has been an Assistant Professor with the Department of Electric, Electronic and Computer Science Engineering, University of Catania. He has 120 scientific publications, mainly in international journals, books, and conference proceedings. His main research activities are in the area of robust audio and speech signal classification and recognition, variable bit-rate speech coding, and adaptive-rate voice and dual stream transmission for mobile IP telephony applications, QoS in mobile Internet access, and drone communications His research interests also include the field of biometric identification and cardiac signal processing and rainfall estimation.

GIACOMO CAPIZZI received the Laurea degree *(summa cum laude)* in electronic engineering from the University of Catania, Catania, Italy, in 1993, and the Ph.D. degree in electronic and computer engineering from the University of Reggio Calabria, Reggio Calabria, Italy, in 2000. From 1993 to 1996, he was a Cabling Systems Designer with Itel (a small company of telecommunications). From 2000 to 2002, he was a Lecturer with the Department of Electrical, Electronics and System Engineering, University of Catania, where he joined as an Assistant Professor in 2002. From 2015 to 2016, from 2016 to 2017, and from 2017 to 2018, he was an Invited Professor with the Silesian University of Technology to teach in a master course on the topic algorithms and paradigms for pattern recognition. His research interests include wavelet theory, neural networks, statistical pattern recognition, Bayesian networks, theory and design of linear and nonlinear digital/analog filters, integrated generation systems, renewable energy sources, and battery storage modeling and simulation.

GRAZIA LO SCIUTO received the Ph.D. degree in applied electronics from the University of Rome Tre in 2016. In 2015, she received the scholarship on the optical calculations for large-scale organic photovoltaic with ENEA-BGU Joint Laboratory, Department of Electrical and Computer Engineering, Ben-Gurion University of the Negev, Israel. Her research interests include electronic devices, semiconducting polymers, organic materials, novel devices for photovoltaic, and neural networks applied to complex systems, such as renewable energy, signal processing, pattern recognition, and biometrics.

CHRISTIAN NAPOLI received the B.Sc. degree in physics, the M.Sc. degree in astrophysics, and the Ph.D. degree in computer science from the Department of Physics and Astronomy, University of Catania, in 2010, 2012, and 2016, respectively. He has been a Student Research Fellow with the Department of Electrical, Electronics and Informatics Engineering, University of Catania, since 2009, a Collaborator of the Astrophysical Observatory of Catania and the National Institute for Nuclear Physics, since 2010, and has been a an Adjunct Professor (since 2015) and Research Fellow (since 2016). He has been several time Invited Professor with the Silesian University of Technology, and Visiting Academic at the New York University. He is currently a Research Associate with the Department of Mathematics and Computer Science. He is the Scientific Director and the Co-Founder of the International School of Advanced and Applied Computing in 2015. He is involved in several international research projects, serves as a reviewer, and is a member of the board program committee for major international journals and international conferences. His current research interests include neural networks, artificial intelligence, computational models, and high performance computing.

FRANCESCO SCAGLIONE received the Laurea degree in telecommunications engineering from the University of Catania in 2011, where he is currently pursuing the Ph.D. degree in electrical, electronic and telecommunications engineering. His research interests include embedded systems, VoIP communications, rainfall estimation, and ICT technologies for environmental control and monitoring.